Thermochimica Acta, 235 (1994) 255–270
Elsevier Science B.V., Amsterdam
SSDI 0040-6031(93)01564-J

A mechanism for the thermal decomposition of potassium permanganate crystals based on nucleation and growth

Michael E. Brown [a], Andrew K. Galwey [b,*], Mohamed A. Mohamed [c] and Haruhiko Tanaka [d]

[a] *Department of Chemistry, Rhodes University, Grahamstown 6140 (South Africa)*
[b] *School of Chemistry, The Queen's University of Belfast, Belfast BT9 5AG (UK)*
[c] *Department of Chemistry, Faculty of Science, Qena (Egypt)*
[d] *Chemistry Laboratory, Faculty of School Education, Hiroshima University, Shinonome, Minami-Ku, Hiroshima 734 (Japan)*

(Received 15 June 1993; accepted 21 August 1993)

Abstract

The mechanism of the thermal decomposition of potassium permanganate crystals is critically reappraised through new microscopic and kinetic observations which are discussed with due consideration of the many and extensive literature reports that relate to this solid state reaction. We identify, from electron micrographs, a crystalline product of unusual texture that is formed early in the reaction. The topography of the residual products of the completely decomposed salt was, however, irregular and no significant textural features were identified. From consideration of the published reports relating to reaction stoichiometry and the chemistry of related reactions, we conclude that the solid products contain material that is inhomogeneous, poorly crystallized and possibly non-stoichiometric.

The decomposition kinetics are shown to be satisfactorily described by the Avrami–Erofe'ev equation ($n = 2$) based on a nucleation-and-growth reaction model. We conclude that permanganate ions decompose in the poorly crystallized zone at the advancing $KMnO_4$/product interface by an electron transfer process, in agreement with a previously published mechanism.

INTRODUCTION

This article reports some highly unusual textural features of product crystallites developed during the solid-state thermal decomposition of potassium permanganate. The textures and dispositions of product in this reactant are of particular interest because it would appear that the reaction mechanism proposed in the early study by Prout and Tompkins [1] has not yet been verified by direct observation. This early study [1] showed that the kinetics of $KMnO_4$ decomposition were well represented by the rate expression now usually referred to as the Prout–Tompkins equation

* Corresponding author.

$$\ln(\alpha/(1-\alpha)) = kt \quad (1)$$

where α is the fractional reaction. The observed autocatalytic characteristics of this decomposition were identified to be a consequence of product formation across the progressively increasing area of reactant surfaces, that resulted from cracking induced by stresses generated at the expanding reactant–product interface [1–3]. We have, however, been unable to find any previous report of a microscopic study of this reaction that provides positive information concerning the textures of the reaction zone participating in $KMnO_4$ decomposition. The present observations may, therefore, be of interest in providing direct evidence concerning the unusual structures of the interface at which the chemical changes occur and in interpreting its extensively investigated kinetic behaviour.

Although there have been several subsequent studies of the kinetics and mechanism of this rate process [4], aspects of its behaviour remain unresolved. For example, the accuracy of fit of isothermal α–time data to the widely used Avrami–Erofe'ev equations [4] have been tested

$$[-\ln(1-\alpha)]^{1/n} = kt \quad (2)$$

These rate expressions, where $n = 2$, 3 or 4, are based on nucleation-and-growth reaction models. It is notoriously difficult to decide whether eqn. (1) or (2) provides the better fit to sets of α–time data [5]. This was pointed out by Brown et al. [6] in considering isothermal DSC data for $KMnO_4$ decomposition, which they found to conform to eqn. (1). Hill et al. [7], in discussing the application of the diffusion-chain mechanism to the same reaction, found that measured α–time values fitted eqn. (1) in the range $0.14 < \alpha < 0.99$, with a single rate constant, although only after a significant initial deviation. Prout and Lownds [8] found that eqn. (1) satisfactorily represented the decomposition of $KMnO_4$, but that eqn. (2) was applicable to reactions of irradiated salt across a restricted α range. Simchen [9] found that $KMnO_4$ decomposition was best described by eqn. (2) with $n = 2$. It is probably realistic to summarize these kinetic analyses by concluding that, except at limiting α values, the differences between the rate equations, eqns. (1) and (2), are too small to permit a clear and unambiguous distinction to be made based on kinetic data alone [5, 6].

There have been disagreements concerning the identities of the crystal phases and the compounds that constitute the solid reaction intermediates and products [10, 11]. Boldyrev [12] has concluded that anion breakdown proceeds through electron transfer steps in the anionic sub-lattice of the reactant.

The present paper describes textures developed during $KMnO_4$ decomposition that we believe have not been reported previously. We also discuss the relevance of these microscopic observations to the kinetic behaviour and to the mechanism of the interface reactions.

RESULTS AND DISCUSSION

Reactant

Reagent grade potassium permanganate, freshly recrystallized from water, was used throughout the present decomposition studies. Reactant samples were composed of small crystallites (dimensions < 1 mm) and some further fragmentation occurred during reaction.

Electron microscopy

Experimental

Reactant samples were decomposed in vacuum to various preselected α values before microscopic examinations of the textures. Crystals were gently crushed, after reaction but before observation, to expose internal features and lightly coated with gold before study in a 35CF Jeol scanning electron microscope. Only features recognized as characteristic and identified in more than a single experiment were photographed.

Introduction

We suggest two possible reasons for the apparent absence from the literature of any description of the structures of the $KMnO_4$ decomposition solid products. Firstly, the small sizes of the product particles are well below the limits of resolution by optical microscopy so that texture identifications require the scanning electron microscope (not available to the early workers). Secondly, the topological features that we describe below, ascribed to reaction, are often obscured by a thin outer surface layer that tends to remain unchanged during reaction. This superficial "skin" may be the result of surface reaction before the onset of the thermal decomposition, an explanation that appears inherently more probable than a lack of surface textural modification during the main reaction. A similar persistent thin (skin-like) superficial layer, that also obscured intracrystalline textural changes, was described in studies of $CsMnO_4$ decomposition [13]. The low reactivity of the outer crystal layer in copper(II) malonate decomposition has also been discussed [14]. As in these earlier studies [13, 14], intracrystalline textural features were revealed on particle fragmentation by gentle crushing of salt samples after partial decomposition to appropriate known α values.

The undecomposed $KMnO_4$ reactant was composed of crystallites of a range of sizes and shapes. Most surfaces were planar and no textural features of significance were identified.

Textures of decomposed $KMnO_4$

A thin layer of largely unmodified surface material, thickness 0.1–0.2 μm, partially detached at a damaged edge of a decomposed crystal is seen in Fig. 1. There was evidence that a high proportion of crystal surfaces were

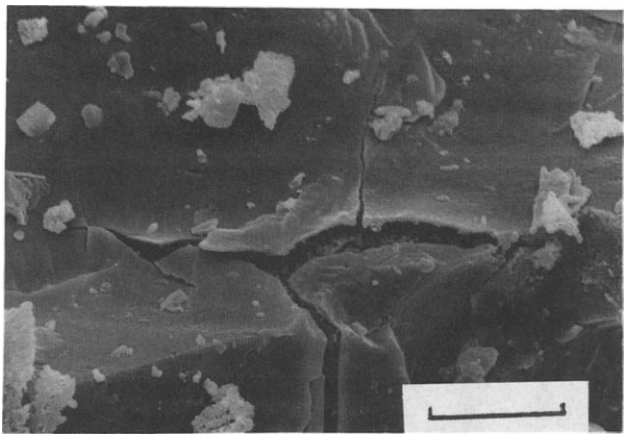

Fig. 1. Scanning electron micrograph of the damaged surface of a decomposed ($\alpha = 1.00$) potassium permanganate crystal. The local detachment of a thin (0.1–0.2 μm), superficial and largely unretextured outer layer is evident. Such outer layers tended to obscure intracrystalline textural modifications that occur during reactions, but could be removed by light crushing after decomposition. Scale bar, 5 μm.

covered by such layers after reactions. However, in all the illustrations reproduced below, such surface layers (where originally present) had been removed to reveal the textural changes accompanying decomposition.

Crystal zones perceived as having undergone local structural modification during reaction and, therefore, recognized as growth nuclei [4], were found in $KMnO_4$ that had been decomposed to $\alpha = 0.10$ and subsequently lightly crushed. Typically, such zones were aggregates of approximately spherical particles, showing no regular or characteristic crystalline structures, Fig. 2,

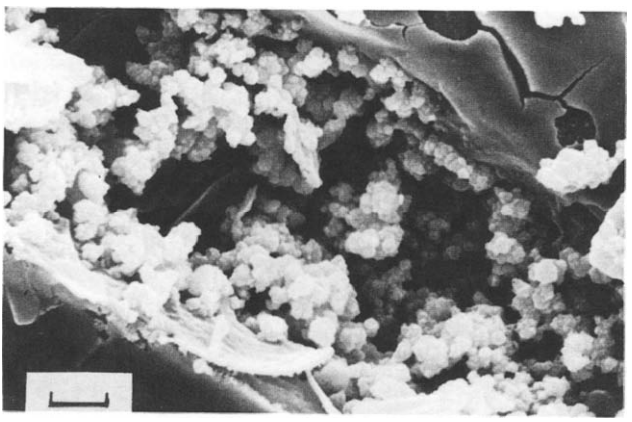

Fig. 2. Scanning electron micrograph of a zone of locally intensively retextured solid in a partially decomposed $KMnO_4$ crystal ($\alpha = 0.10$ at 500 K). Reaction has generated large numbers of irregularly shaped particles. This evidence of preferred reaction zones is indicative of a nucleation-and-growth mechanism. Scale bar, 1.0 μm.

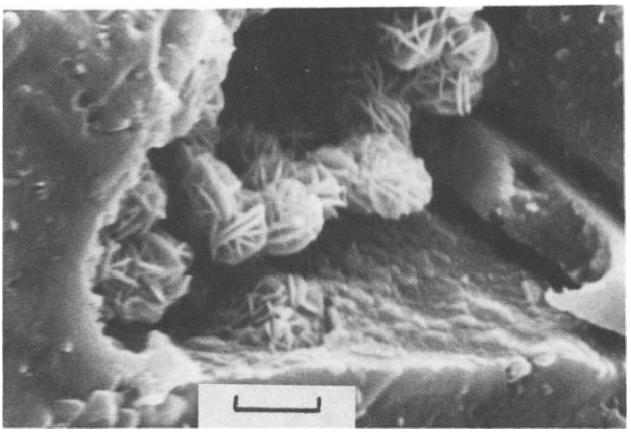

Fig. 3. On another crystallite from the same decomposition experiment as Fig. 2 ($\alpha = 0.10$ at 500 K), growth nuclei developed as this highly characteristic product texture. Product appears as approximately spherical particles composed of coherent short acicular crystals. In the upper portion of the micrograph there is evidence of reactant recrystallization/reorganization at the reaction interface. Scale bar, 1.0 μm.

or consisted of approximately spherical aggregates (up to approx. 1 μm in diameter) of acicular components, Fig. 3. The textures shown in Figs. 2 and 3 were found in the same experiment, while those shown in Fig. 4 were from the same batch of prepared salt but in a different experiment. Further examples of similar textures developed in another salt preparation are shown in Figs. 5a and 5b, though here the same individual components of the texture were aggregated into more extended asymmetric groupings. In a further experiment, in which $KMnO_4$ was decomposed to $\alpha = 0.05$ (only), there were comparable, but not texturally identical, spheres each of which was located in a pit, probably representing the volume of reactant from which it was derived, Figs. 6a and 6b.

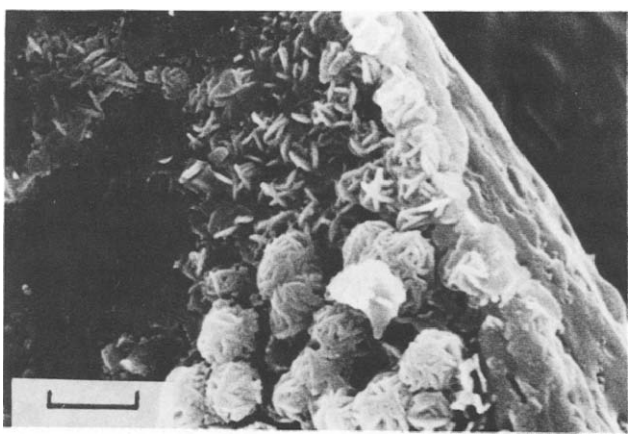

Fig. 4. Textures similar to those in Fig. 3, obtained in a different experiment, again to $\alpha = 0.10$ at 500 K. Scale bar, 1.0 μm.

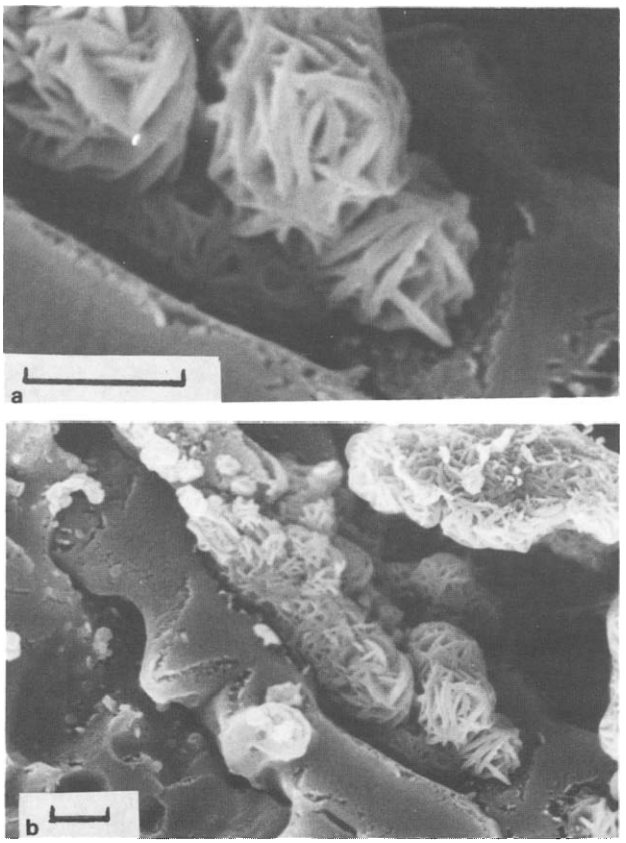

Fig. 5a and b. Further examples of product textures, similar to but showing points of difference from those in Figs. 3 and 4 (again $\alpha = 0.10$ at 500 K). There were some individual spherical aggregates (a) but there was also evidence of greater coalescence of similar constituent crystals to form more extended, asymmetric groupings elsewhere in the same nucleus. Scale bars, both 1.0 μm.

We found no unifying feature that characterized the products of extensive ($\alpha > 0.7$) or completed ($\alpha = 1.00$) $KMnO_4$ decomposition. The variety and irregularity of the surface topography defy brief, or indeed meaningful, description. Crystals undergo some fragmentation during reaction, but this was not extensive and did not result in comprehensive particle disintegration. Residual products included particles that were of a wide variety of shapes and sizes, similar to those of the original reactant. These included generally flat faces similar to those of the original solution-grown crystals, though reaction generated smaller surface irregularities. Pores and faces were sometimes distorted by numerous small protuberances. Other areas of product particles resembled, to some extent, those in Figs. 6a and 6b in which there were rounded particles and a pitted but coherent matrix. No indication of the highly characteristic textures shown in Figs. 3–5 could, however, be found. Many other textures were observed, but these were not

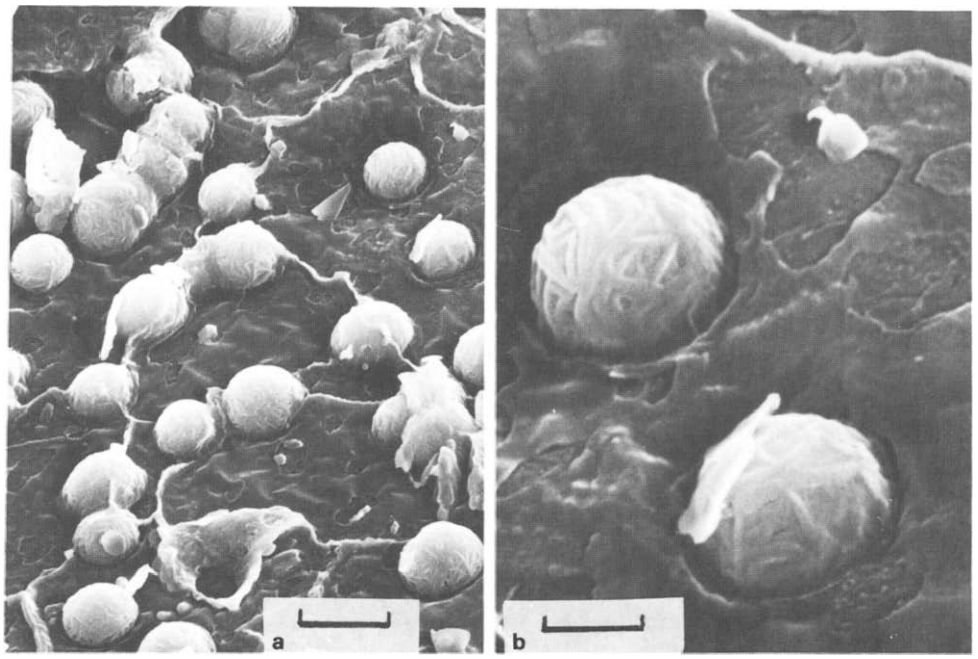

Fig. 6a and b. In another experiment ($\alpha = 0.05$ at 500 K), the spherical aggregates were more perfect and each was located in a pit. This structure was observed only in areas from which the original covering layer had been removed. Scale bars; a, 3.0 μm; and b, 1.0 μm.

general and were too varied to permit useful description. The only novel features discerned at high α values were fibrous structures of the type shown in Fig. 7. These were seen in only a few locations and show smooth surfaces with irregularities of shape that are reminiscent of plastically deformed structures.

There is the possibility that the textures shown in Figs. 2–5 are composed of the intermediate $K_3[MnO_4]_2$ [11, 12] that undergoes subsequent decomposition with consequent loss of this structure from the final residual product.

Comment

From the above observations we conclude that, at least in the early stages, the solid state decomposition of $KMnO_4$ proceeds with the participation of a nucleation-and-growth mechanism for the following reasons.

(i) There was no evidence that decomposition is accompanied by significant melting. Residual crystallites usually appear to be pseudo-morphic with those of the reactant and there was no evidence of intracrystalline froth formation, as in copper(II) malonate decomposition [14]. The product textures shown in the figures are composed of components having flat faces and sharp angles between faces, characteristic features of crystals.

(ii) Product formation in local aggregates, Figs. 2–6, is characteristic of the nucleation-and-growth model. Observational evidence supporting this

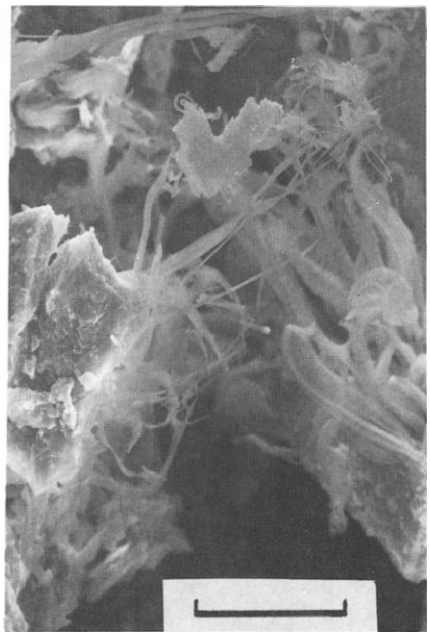

Fig. 7. Textures of decomposed $KMnO_4$ were irregular, see text. In the residual product ($\alpha = 1.00$ at 500 K) there were a few local examples of the fibrous-type structure seen here, in which the fibres showed smooth sufaces and were often bent. Several examples of such structures were observed but this material constituted only a very small fraction of the residue. Scale bar, 10 μm.

reaction mechanism has not previously been provided, possibly because structures of the type described here have been obscured by the superficial unretextured layer. It is appropriate, therefore, to test obedience of isothermal kinetic data for $KMnO_4$ decomposition for fit to the Avrami–Erofe'ev equations, applicable to such reactions. This is reported in the following section.

Reaction kinetics

Reactant

Kinetic measurements were carried out using the same salt preparations as those studied in the microscopic examinations to permit meaningful comparisons between the two types of observation.

Apparatus

Reactant samples (approx. 50 mg weighed ± 0.2 mg) were decomposed in a conventional glass vacuum apparatus, initially evacuated for 1 h at $< 10^{-4}$ Torr. Each salt specimen, in a small glass tube, was, after isolation from the pumps, admitted to the constant temperature (± 0.7 K) reaction zone. During most kinetic studies (except those proceeding in a small

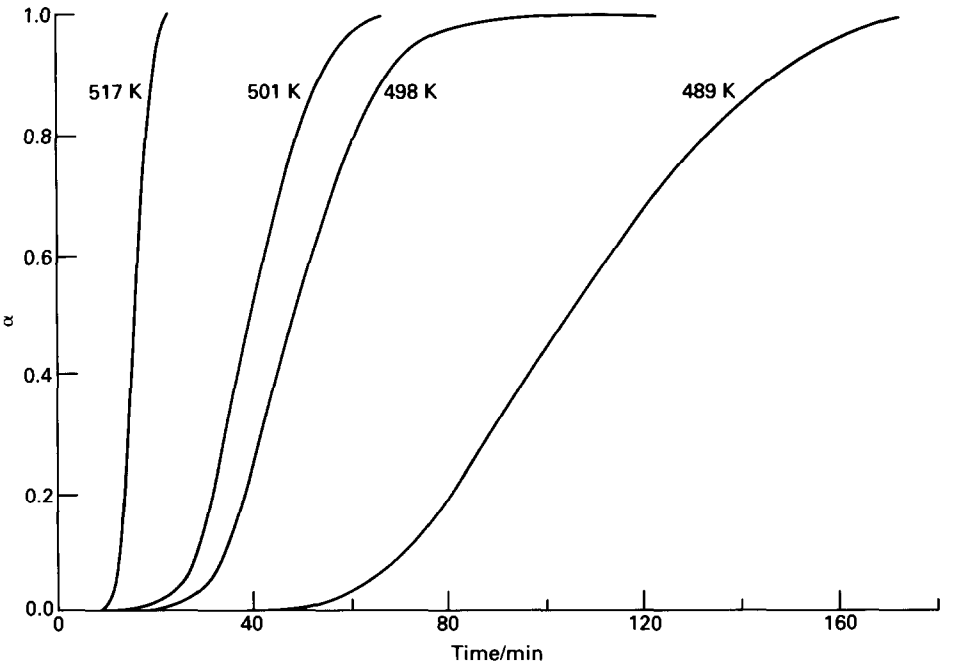

Fig. 8. Typical α–time plots for the isothermal decomposition of recrystallized $KMnO_4$ at four representative temperatures. The characteristic sigmoid curves are similar to behaviour reported in previous studies.

pressure of water vapour), a 78 K cold trap was maintained between reactant and a Baratron absolute pressure diaphragm gauge used to measure (between 0 and 10 Torr, accuracy ± 0.001 Torr) the pressure of oxygen gas evolved by $KMnO_4$ breakdown. A computer, interfaced with the pressure gauge and with a thermocouple located beside the reactant salt, recorded the pressure of oxygen product and the reactant temperature at specified time intervals. Data (time, temperature, pressure values) were stored in the computer memory for later analysis. Pressure data were converted to α values and the fit of yield–time data to the rate equations used in kinetic analyses of solid state decompositions was tested [4]. Calculated values could be printed in appropriate graphical forms or in tables to permit the rate expression most satisfactorily [5] representing the observations to be identified. A more detailed description of the apparatus has already been published [14].

Kinetic analysis

Crystals grown from solution. Plots of α against time for the isothermal decomposition of $KMnO_4$ crystals grown from aqueous solution were sigmoid, agreeing with previous work [1]: typical examples are shown in Fig. 8. These, and all our comparable measurements, were very satisfactorily represented by eqn. (2), $n = 2$, across the mean range $0.03 < \alpha < 0.97$. This is shown by the extended linear regions of the plots in Fig. 9 for the

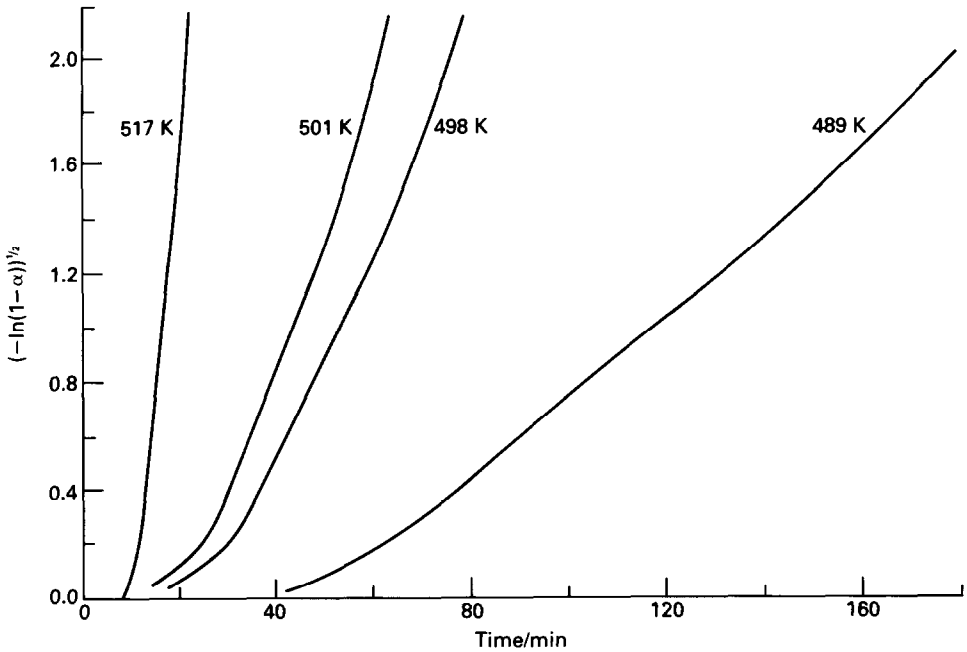

Fig. 9. Plots of $[-\ln(1-\alpha)]^{1/2}$ against time for the data in Fig. 8: the mean range of the linear regions was $0.03 < \alpha < 0.97$. The deviations at limiting α-values are discussed in the text.

data from Fig. 8. The linearity of the Prout–Tompkins plots, eqn. (1), was, however, very much less satisfactory, as shown in Fig. 10, again using the data from Fig. 8. The reactivities of two similar salt preparations were identical and all rate constants, eqn. (2), $n = 2$, were close to a single line on an Arrhenius plot from which the calculated activation energy was 165 ± 10 kJ mol^{-1} for data between 465 and 520 K. This value is close to that (161 kJ mol^{-1}) reported by Prout and Tompkins [1] for the same reaction. The fits of data to eqn. (2), with $n = 3$ or 4, were less satisfactory, particularly at low α values, and plots were linear only when $\alpha > 0.2$.

The decompositions of the crystals were preceded by an appreciable induction period. The subsequent onset of reaction was acceleratory when $\alpha > 0.03$, as is evident from Fig. 8. Rates when $\alpha > 0.97$ were very sensitive to the value of the final pressure used to calculate α; this was difficult to determine precisely because of a very slow final rate of oxygen evolution. Despite these deviations at the limits, the fit of data to eqn. (2), $n = 2$, was most satisfactory. This is interesting because of the acceptable description of the kinetics of this reaction by a rate equation based on a nucleation-and-growth reaction model.

Crushed crystals. Pre-crushing the reactant crystals resulted in relatively minor modifications in the kinetic characteristics of subsequent decomposition. This is evident from the representative α–time curves in Fig. 11 for

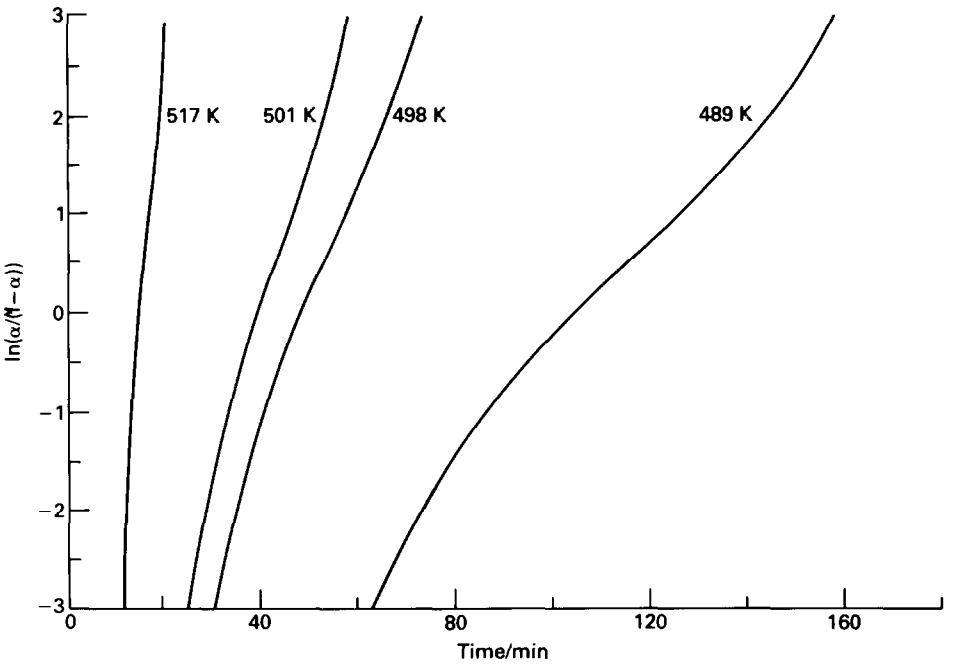

Fig. 10. Plots of $\ln(\alpha/(1-\alpha))$ against time for the data in Fig. 8: the linearity of these plots is very much less satisfactory than that of Fig. 9. The Avrami–Erofe'ev equation provides a more satisfactory fit to the data overall than the Prout–Tompkins equation.

reactions at 498 ± 1 K. Crushing appreciably decreased, but did not eliminate, the induction period to onset of a reaction that initially ($\alpha < 0.2$) developed relatively more rapidly than in uncrushed crystals. These data again fitted eqn. (2), but here with $n = 3$ or 4 rather than with $n = 2$; kinetic behaviour was influenced by the sizes and shapes of reactant particles, changed by the mechanical pretreatment. Typical differences in rate characteristics are shown in Fig. 11. Rate constants obtained from the (less satisfactory) eqn. (2), $n = 2$, plots were on the same line as the Arrhenius plot for the crystalline reactant. Slopes of the α–time graphs can be seen to be closely similar in the median α-region. The calculated activation energy was again 165 ± 10 kJ mol^{-1}. We did not confirm a decrease in activation energy (to 140 kJ mol^{-1}) on crushing, as has been reported previously [1].

Crystals decomposed in water vapour. Crystal decompositions in small pressures of water vapour, 2.0–3.5 Torr H_2O, were identical, within experimental error, with those of the dry reaction, Fig. 11. Again eqn. (2), $n = 2$, fitted the data across the same α range, $0.03 < \alpha < 0.97$, and rate constants were on the same line on the Arrhenius plot as reactions with the cold trap. The only consequence of the presence of water vapour was a small decrease in the induction period.

These experiments were performed to investigate the possibility that the reaction might proceed more rapidly through the intervention of perman-

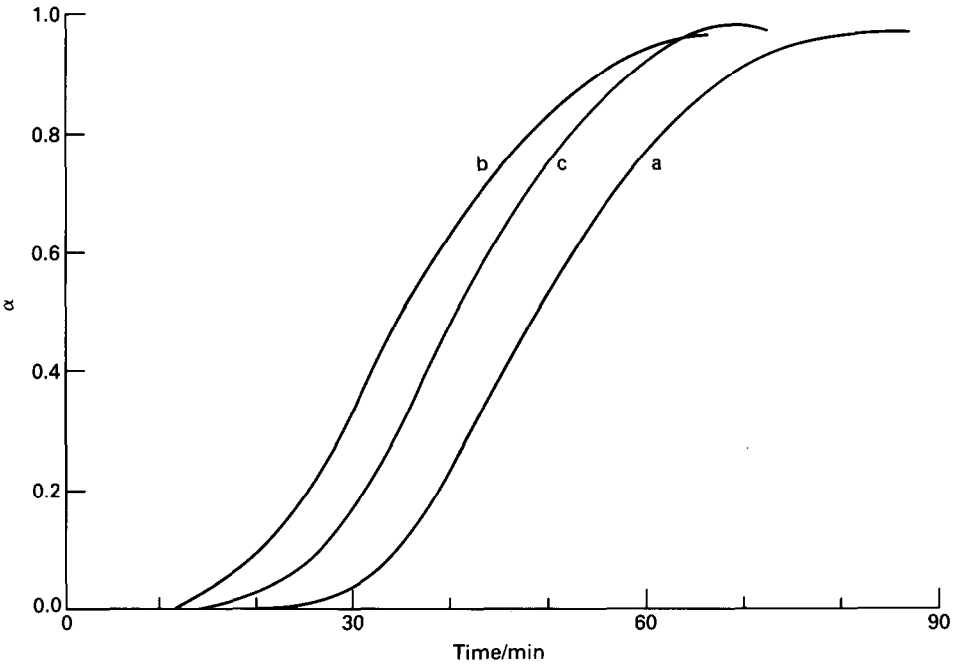

Fig. 11. Comparison of α–time plots for $KMnO_4$ decompositions at 498 K of three reaction systems: curve a, recrystallized salt (last reaction to start); curve b, crushed salt (first reaction to start); and curve c, salt decomposed in 3.0 Torr water vapour (middle reaction).

ganic acid as an intermediate. Clearly our results provide no support for such a mechanism.

Distinguishability of sigmoid models

A reference set of (α, t) values was generated from the Prout–Tompkins (B1) equation with $k_B = 0.03892\ s^{-1}$ and $t_0 = -200$ s. The value of k_B was chosen so that $\alpha = 0.98$ at $(t - t_0) = 100$ s. These (α, t) values were then analysed for kinetic fit to the Avrami–Erofe'ev (An) models (with $n = 2$, 3 and 4) over the range $0.02 < \alpha < 0.98$. The values of k_A and t_0 obtained and the r^2 values for linear regression analyses are given in Table 1. The A4 model gives the closest fit [5]. The analysis was reversed by using the k_A values from Table 1 to calculate sets of (α, t) values for eqn. (2) $n = 2$, 3 and 4, and then analysing these sets for fit to the B1 model. The values of k_B and t_0 obtained are included in Table 1 and confirm the difficulty in distinguishing meaningfully between the applicability to a given set of (α, t) values of the Prout–Tompkins equation (B1) and the Avrami–Erofe'ev equation (An), particularly when $n = 4$. This problem, demonstrated here for idealised data, is more difficult to resolve in practical kinetic analyses of real systems because of the contributions from experimental uncertainties [5].

TABLE 1

Comparison of the applicability of the Prout–Tompkins equation (B1) and the Avrami–Erofe'ev equations (An) to ideal sets of data ($0.02 < \alpha < 0.98$)

	Model	k/s^{-1}	t_0/s	r^2
Input	B1	0.03892	−200	1.000
Output	A2	0.009848	−106.1	0.9804
Output	A3	0.006940	−70.52	0.9952
Output	A4	0.005494	−35.84	0.9962
Input	A2	0.009848	0	1.000
Output	B1	0.03587	−90.7	0.9885
Input	A3	0.006940	0	1.000
Output	B1	0.03816	−129.1	0.9948
Input	A4	0.005494	0	1.000
Output	B1	0.03883	−164.0	0.9949

Reaction mechanism

As pointed out previously [15], mechanistic analyses of solid-state reactions require complementary consideration of two features of the advancing reactant–product interface: (i) the geometry of interface development, usually deduced from the rate equation found to apply, together with microscopic observations; and (ii) the chemical steps through which reactant species are converted into products; evidence can be obtained from microscopy, together with the stoichiometry and possibly the magnitude of the activation energy.

Kinetic analysis

Both kinetic analyses (the extended range of fit by eqn. (2), $n = 2$) and microscopic observations provide direct evidence that the $KMnO_4$ decomposition proceeds by a nucleation-and-growth mechanism. It is undoubtably difficult to distinguish this close fit from that of eqn. (1) [5, 6]. However, this extended applicability of a single rate constant ($0.03 < \alpha < 0.97$, representing 94% of reaction) is preferable to the two linear regions [1], often joined by a curved interval, that are frequently seen in Prout–Tompkins plots for this reaction.

Crushing resulted in no detectable change in reaction rate except for the diminution of the induction period. From theoretical considerations [4] it can be expected that the increase in reactant surface could result in an increase in the number of nuclei generated. However, if nucleus growth is restricted to the individual particle on which it appears, then this effect will result in a decrease in rate on crushing. Although these effects are in opposite directions, it is considered to be inherently improbable that they will exactly cancel, as required to explain the observed behaviour. An

alternative, and preferred, interpretation is that the number of specialized nucleation sites in the original crystallites is not significantly changed on cold working and that a growth nucleus is capable of developing from one crystallite to a neighbour with which it is in contact. A similar mechanism of extended nucleus growth in powders has already been proposed to explain the kinetics of dehydration of D-lithium potassium tartrate monohydrate [16]. The product phase is regarded as providing a seed crystal for the difficult recrystallization step, thereby promoting the advance of reaction from one crystal to another that it touches. This reaction model can be expected to result in kinetic obedience to the Avrami–Erofe'ev equation, eqn. (2).

Reaction stoichiometry

A critical consideration of the analytical evidence relating to the $KMnO_4$ decomposition reveals no data that establish conclusively the stoichiometry of this reaction. Prout and Tompkins [1] found that their results were fairly well expressed by

$$2KMnO_4 \rightarrow K_2MnO_4 + MnO_2 + O_2$$

though the solids were not characterized and the average oxygen yields were $0.98-1.06O_2$. The presence of K_2MnO_4 as a residual product has since been characterized by X-ray diffraction [10, 11], although the enhanced scattering background indicates the presence of other poorly crystallized material [11]. The intermediate production of $K_3[MnO_4]_2$ below 488 K has also been reported [11] due to ready reaction in the crystalline material of $MnO_4^{2-} \rightleftharpoons MnO_4^-$ [17].

The most extensive examinations of the residual solids have been reported by Herbstein et al. [10]

$$10KMnO_4 \rightarrow 2.65K_2MnO_4 + (2.35K_2O \cdot 7.35MnO_{2.05}) + 6O_2 \quad (3)$$

where the elements in parentheses are described as 'a crypto-melanc-like material whose composition and structure are not known at present' [10]. This is referred to by the "non-committal label" '$K_4Mn_7O_{16}$' which (surprisingly) does not accurately represent the elemental balance, as can be seen from the alternative presentation of eqn. (3)

$$10KMnO_4 \rightarrow 2.65K_2MnO_4 + 1.18(K_{4.00}Mn_{6.25}O_{14.02}) + 6O_2$$

Bearing in mind the problems encountered in characterizing the structures and compositions of manganese oxides [18] and in elucidating the chemistry of their reactions with potassium oxide [19], we emphasize the uncertainties that remain in elucidating the compositions and structures of the compounds that constitute the residual decomposition products of $KMnO_4$. It seems improbable that these have fully crystallized at the reaction temperature, because reactions of KOH + manganese oxides proceeded at temperatures above 575 K [19].

We regard as significant the differences in reported oxygen yields from $2KMnO_4$, namely $1.0O_2$ [1] and $1.2O_2$ [10]. The latter is not consistent with the high-oxygen component $MnO_{2.05}$ in eqn. (3) [10], which can also be expressed (to emphasize the constituents as mainly Mn^{6+} and Mn^{3+}) as

$$10KMnO_4 \rightarrow 5K_2MnO_4 + 5MnO_{1.6} + 6O_2 \quad (4)$$

These results can be compared with oxygen yields reported for other alkali permanganates: $2RbMnO_4$ yields $1.2O_2$ [10] and $1.24O_2$ [20], and $2CsMnO_4$ yields $1.4O_2$ [21] and $1.0O_2$ [12].

We conclude that the oxygen yield and, therefore, the oxidation states of manganese in the products of $KMnO_4$ decomposition have not been accurately measured. Whereas K_2MnO_4 product and $K_3(MnO_4)_2$ intermediate have been identified, a high proportion of the residue remains uncharacterized. It seems unlikely that this portion is crystalline or composed of any well-defined stoichiometric product, but can be more realistically regarded as amorphous and inhomogeneous. Higher temperatures (>575 K, [19]) may be required to enable reactions and recrystallization to proceed to completion. These considerations account for the detection, during microscopy, of *some* crystalline products. However, the observation that the textures of the final residues were poorly defined, irregular and inhomogeneous is entirely consistent with the stoichiometric uncertainties and the properties of the oxides of manganese.

Interface reactions

From the above kinetic analyses we conclude that $KMnO_4$ decomposition occurs at a reaction interfacial zone that progresses through reactant crystallites by a nucleation-and-growth mechanism [4]. The advance of this interface cannot, however, be supported by direct observational evidence, because there was no textural feature that could be reliably used to distinguish between the reactant and the solid products. There was evidence that the product was heterogeneous, poorly crystallized and composed of more than one phase.

We conclude, therefore, that the chemical changes of the permanganate ion occur after its transfer from the stabilizing structure of the reactant solid ($KMnO_4$) into the more disorganized environment of the product assemblage. Reaction is satisfactorily explained by electron transfer [17] followed by oxygen elimination, as suggested by Boldyrev [12]

$$2MnO_4^- \rightleftharpoons MnO_4^{2-} + MnO_4^{\cdot} \rightarrow MnO_4^{2-} + MnO_2 + O_2$$

at, or close to, the active interface. The elimination of an oxygen molecule and accommodation of the species MnO_4^{2-} and MnO_2 into the solid products are undoubtedly more complicated than is implied here.

The accompanying changes of lattice order may result in reactant cracking of the type envisaged by Prout and Tompkins [1]. If disintegration

occurs, it must be followed by product interactions to form the residual coherent particles of solid that are often pseudo-morphic with those of reactant. Microscopic studies gave no evidence that $KMnO_4$ decomposition resulted in extensive breakup of crystals.

The mechanism described above is consistent with the generalization that the calculated activation energies for the decompositions of $KMnO_4$, $RbMnO_4$ and $CsMnO_4$ [1, 13, 20–22] are of similar magnitudes, approx. 160–170 kJ mol^{-1}. (Values for the lithium and sodium salts were somewhat lower, approx. 135 kJ mol^{-1} [22].) This constancy is consistent with the view that neither cation, nor crystal structure, nor crystal stability exerts significant influence upon the anion breakdown step. Reaction is envisaged as occurring within the disorganized layer where electron transfer between anions may be facilitated. Additives which promote such electron transfer catalyse the $KMnO_4$ decomposition [23].

REFERENCES

1 E.G. Prout and F.C. Tompkins, Trans. Faraday Soc., 40 (1944) 488.
2 D.A. Young, Decomposition of Solids, Pergamon Press, Oxford, 1966.
3 F.C. Tompkins, Treatise on Solid State Chemistry, in N.B. Hannay (Ed.), Reactivity of Solids, Vol. 4, Plenum Press, New York, 1976, Chapt. 4.
4 M.E. Brown, D. Dollimore and A.K. Galwey, Comprehensive Chemical Kinetics, Vol. 22, Elsevier, Amsterdam, 1980.
5 M.E. Brown and A.K. Galwey, Thermochim. Acta, 29 (1979) 129.
6 M.E. Brown, K.C. Sole and M.W. Beck, Thermochim. Acta, 89 (1985) 27; 92 (1985) 149.
7 R.A.W. Hill, R.T. Richardson and B.W. Rodger, Proc. R. Soc. London Ser. A, 291 (1966) 208.
8 E.G. Prout and C.M. Lownds, Inorg. Nucl. Chem. Lett., 9 (1973) 617.
9 A.E. Simchen, J. Chim. Phys., (1961) 596.
10 F.H. Herbstein, G. Ron and A. Weissman, J. Chem. Soc. A, (1971) 1821; see also, (1973) 1701.
11 V.V. Boldyrev, A.P. Voronin, T.A. Nevolina and V.V. Marusin, J. Solid State Chem., 20 (1977) 327.
12 V.V. Boldyrev, J. Phys. Chem. Solids, 30 (1969) 1215.
13 A.K. Galwey and S.A.A. Mansour, Thermochim. Acta, 228 (1993) 379.
14 N.J. Carr and A.K. Galwey, Proc. R. Soc. London Ser. A, 404 (1986) 101.
15 A.K. Galwey, Thermochim. Acta, 96 (1985) 259; React. Solids, 8 (1990) 211.
16 A.K. Galwey, G.M. Laverty, N.A. Baranov and V.B. Okhotnikov, Philos. Trans. R. Soc. (London), in press.
17 B.G. Erenburg, L.N. Senchenko, V.V. Boldyrev and A.V. Malysh, Russ. J. Inorg. Chem., 17 (1972) 1121.
18 T.E. Moore, M. Ellis and P.W. Selwood, J. Am. Chem. Soc., 72 (1950) 852.
19 G.A. El-Shobaky, K.A. El-Barawy and A.A. Ibrahim, Thermochim. Acta, 102 (1986) 21.
20 P.J. Herley and E.G. Prout, J. Phys. Chem., 64 (1960) 675; J. Inorg. Nucl. Chem., 16 (1960) 16.
21 P.J. Herley and E.G. Prout, J. Chem. Soc., (1959) 3300.
22 E.G. Prout and P.J. Herley, J. Phys. Chem., 66 (1962) 961.
23 E.A. Hassan, A.A. Said and K.M. Abd El-Salaam, Thermochim. Acta, 91 (1985) 9; 38 (1980) 271.